HEPATOLOGY
Official Journal of the American Association for the Study of Liver Diseases

Elastin Accumulation Is Regulated at the Level of Degradation by Macrophage Metalloelastase (MMP-12) During Experimental Liver Fibrosis

Antonella Pellicoro,[1] Rebecca L. Aucott,[1] Prakash Ramachandran,[1] Andrew J. Robson,[1] Jonathan A. Fallowfield,[1] Victoria K. Snowdon,[1] Stephen N. Hartland,[1] Madeleine Vernon,[1] Jeremy S. Duffield,[2] R. Christopher Benyon,[3] Stuart J. Forbes,[1,4] and John P. Iredale[1]

Elastin has been linked to maturity of liver fibrosis. To date, the regulation of elastin secretion and its degradation in liver fibrosis has not been characterized. The aim of this work was to define elastin accumulation and the role of the paradigm elastase macrophage metalloelastase (MMP-12) in its turnover during fibrosis. Liver fibrosis was induced by either intraperitoneal injections of carbon tetrachloride (CCl_4) for up to 12 weeks (rat and mouse) or oral administration of thioacetamide (TAA) for 1 year (mouse). Elastin synthesis, deposition, and degradation were investigated by immunohistochemistry, quantitative polymerase chain reaction (qPCR), western blotting, and casein zymography. The regulation of MMP-12 elastin degradation was defined mechanistically using CD11b-DTR and MMP-12 knockout mice. In a CCl_4 model of fibrosis in rat, elastin deposition was significantly increased only in advanced fibrosis. Tropoelastin expression increased with duration of injury. MMP-12 protein levels were only modestly changed and in coimmunoprecipitation experiments MMP-12 was bound in greater quantities to its inhibitor TIMP-1 in advanced versus early fibrosis. Immunohistochemistry and macrophage depletion experiments indicated that macrophages were the sole source of MMP-12. Exposure of CCl_4 in MMP-$12^{-/-}$ mice led to a similar degree of overall fibrosis compared to wildtype (WT) but increased perisinusoidal elastin. Conversely, oral administration of TAA caused both higher elastin accumulation and higher fibrosis in MMP-$12^{-/-}$ mice compared with WT. *Conclusion*: Elastin is regulated at the level of degradation during liver fibrosis. Macrophage-derived MMP-12 regulates elastin degradation even in progressive experimental liver fibrosis. These observations have important implications for the design of antifibrotic therapies. (HEPATOLOGY 2012;55:1965-1975)

Abbreviations: CCl_4, carbon tetrachloride; HSC, hepatic stellate cell; LOX, lysyl-oxidase; MMP, macrophage metalloelastase; NE, neutrophil elastase; TAA, thioacetamide; TIMP, tissue inhibitors of metalloproteinase; tTG, tissue transglutaminase; WT, wildtype.

From the [1]MRC/UoE Centre for Inflammation Research, University of Edinburgh, Edinburgh, UK; [2]Division of Nephrology, Department of Medicine, University of Washington, Institute for Stem Cell and Regenerative Medicine, Seattle, WA; [3]Liver and Pancreas Group, University of Southampton, Division of Infection, Inflammation and Immunity, Southampton General Hospital, Southampton, UK; and [4]MRC Centre for Regenerative Medicine, Edinburgh, UK.

Received June 16, 2011; accepted December 13, 2011.

fax: 0131 242 6578

Address reprint requests to: Antonella Pellicoro, MRC/UoE Centre for Inflammation Research, University of Edinburgh, 47 Little France Crescent, Edinburgh, EH16 4TJ, UK. E-mail: apellico@staffmail.ed.ac.uk; fax: 0131 242 6578.

Copyright © 2012 by the American Association for the Study of Liver Diseases.

View this article online at wileyonlinelibrary.com.

DOI 10.1002/hep.25567

Potential conflict of interest: Nothing to report.

Additional Supporting Information may be found in the online version of this article.

Liver fibrosis and its endstage, cirrhosis, represent a major worldwide health problem.[1] Although removal of the underlying injurious process (e.g., with antiviral therapy) may halt the progression of liver fibrosis, liver transplantation remains the only effective treatment for advanced fibrosis and cirrhosis. Unfortunately, the limited supply of donor organs restricts the availability of this treatment.

In recent years, studies in rodents[2-4] corroborated by sequential study of human liver cirrhosis[5] have led to a paradigm shift in the understanding of fibrosis reversibility: both advanced fibrosis and cirrhosis, previously considered irreversible, are at least partly reversible following withdrawal of the injurious stimulus.

The development of liver fibrosis is associated with profound changes in both the biochemical composition

and physical properties of the extracellular matrix. It is now clear that hepatic stellate cells (HSCs) are a major contributor to hepatic myofibroblasts, which represent the key effector cell population in the development of fibrosis, secreting fibrillar collagens and other matrix components, including elastin.[6-8] Despite the concurrent expression of matrix degrading metalloproteinases (MMPs), net matrix accumulation occurs in the injured liver, in major part as a result of expression of the potent tissue inhibitors of metalloproteinases (TIMPs 1 and 2) by HSC.[9,10]

Previous fibrosis studies have focused almost exclusively on secretion and turnover of collagens. However, other matrix components play critical roles in the development and progression of fibrosis. Elastin is the main component of elastic fibers, together with amorphous components, in particular fibrillin and microfibrillar-associated proteins including fibulins and Emilin-I.[11,12] Elastin is an insoluble nonpolar protein, formed by polymerization of the soluble monomer tropoelastin.[13] The tropoelastin molecule is rich in alanine and lysine residues, which are principal sites for crosslinking reactions. Such reactions are potentially catalyzed by either lysyl-oxidase (LOX) or tissue transglutaminase (tTG)[14,15]; in addition, in mature scars a nonenzymatic reaction is possible.[11] Thus, intermolecular crosslinks increase the insolubility of the elastic fibers and render matrix resistant to degradation, in turn limiting the reversibility of fibrosis.

Elastic fibers are present in the normal liver in the capsule and portal tracts and their number increases in fibrosis and cirrhosis.[16,17] Furthermore, the ratio between elastin and collagen increases as liver fibrosis progresses.[18] In parallel, an increase in crosslinking is observed.[19] Despite this clear contribution of elastin to liver fibrosis and progression of liver disease, the regulation of elastin secretion and turnover has not been investigated in liver fibrosis.

Two main cell types are responsible for elastin degradation, neutrophils, secreting neutrophil elastase (NE), and macrophages through macrophage metalloelastase (MMP-12).[20] Like other MMPs, MMP-12 is transcriptionally regulated,[21] secreted as a proenzyme, and subsequently activated by (self)-cleavage in the extracellular space.

Macrophage depletion during spontaneous recovery from fibrosis leads to a failure of matrix degradation, associated with an increase in scar elastin relative to control[22] (see below). This suggests that macrophages serve a discrete function mediating degradation of elastin. Furthermore, Fallowfield et al.[23] have shown expression of MMP-13 (collagenase 3) by scar-associated macrophages, suggesting that these cells may be critically important in mediating matrix remodeling during fibrosis.

We therefore deployed targeted gene mutation and conditional macrophage depletion studies to define the role of macrophages and MMP-12 in mediating elastin turnover during progressive fibrosis. Our data provide evidence that elastin is regulated at the level of degradation during experimental liver fibrosis. Specifically, macrophage-derived MMP-12 appears to be critical for regulating elastin degradation in progressive experimental liver fibrosis.

Materials and Methods

Animals. Animals were housed in standard sterile conditions with free access to chow and water. All procedures were undertaken in accordance with the local ethical committee.

Progressive Rat Liver Fibrosis. Carbon tetrachloride (CCl_4) liver injury was induced as described[24] for a total of 4, 8, and 12 weeks to generate fibrosis and early and established cirrhosis, respectively.

Murine Model of Hepatic Fibrosis in CD11b-DTR-Transgenic Mice. Generation of the CD11b-DTR mice was described.[22,23] In brief, adult CD11b-DTR mice (FVB/N) were injected with 0.25 μL/g CCl_4 intraperitoneally twice weekly for 12 weeks. During the final week the mice were given either diphtheria toxin (DT 25 ng/g intraperitoneal) or phosphate-buffered saline (PBS) immediately after the first injection of CCl_4 that week, 24 hours later, and an additional 48 hours later to coincide with the last injection of CCl_4.

Short Murine Model of Hepatic Fibrosis and Macrophage Isolation. C57Bl/6 mice were injected with either CCl_4 (0.4 μL/g) mixed 1:3 with olive oil or olive oil alone for 4 weeks. Livers were harvested at 48 hours after the final injection of CCl_4. Upon harvest all livers were perfused with saline solution before being enzymatically digested using collagenase B (1.6 mg/mL) and DNase I (100 μg/mL) (Roche, UK). Samples were then passed through a 40-μm cell strainer and subjected to red blood cells lysis (150 mM NH_4Cl, 10 mM $KHCO_2$, 0.1 mM EDTA). Cells were counted and labeled with F4/80-APC antibody (0.5 μL / 1 $\times$ 10^6 cells) (Caltag, UK) before positive, immunobead, magnetic selection using anti-APC beads (2.5 μL / 1 $\times$ 10^6 cells) (Caltag, UK). Cells from macrophage-enriched and depleted populations were then placed in Trizol (Invitrogen, UK) and stored at -80°C for subsequent analysis.

15273350, 2012, 6, Downloaded from https://onlinelibrary.wiley.com/doi/10.1002/hep.25567, Wiley Online Library on [24/10/2025]. See the Terms and Conditions (https://onlinelibrary.wiley.com/terms-and-conditions) on Wiley Online Library for rules of use; OA articles are governed by the applicable Creative Commons License

MMP-12 Knockout Murine Models of Hepatic Fibrosis. Breeding pairs of MMP-12-deficient mice (MMP-12$^{-/-}$) were purchased from the Jackson Laboratory (Bar Harbor, ME).

Liver fibrosis was induced in cohorts of sex- and age-matched MMP-12$^{-/-}$ and wildtype (WT) C57BL/6 mice by 12 weeks, twice-weekly intraperitoneal administration of either CCl_4 (0.4 μL/g) in olive oil (1:3) or olive oil alone (n = 6 in each group). Animals were euthanized 48 hours after the final dose of CCl_4. Three normal, untreated, mouse livers were also harvested in both MMP-12$^{-/-}$ and WT groups for use as additional controls in individual experiments.

Alternatively, liver fibrosis was induced in cohorts of sex- and age-matched MMP-12$^{-/-}$ and WT C57BL/6 mice by administration of thioacetamide (TAA; 600 mg/L) in drinking water for 1 year.

In both models, animals were sacrificed together with age- and sex-matched controls and livers were split and fixed in either formalin or methacarn for subsequent immunohistochemical studies or snap-frozen in liquid nitrogen for biochemical and molecular analysis.

Human Monocytes Derived Macrophages. Human peripheral blood mononuclear cells were isolated by dextran sedimentation and centrifugation using a Percoll gradient and monocyte-derived macrophages were derived as described.[25]

Immunohistochemistry and Immunocytochemistry. Assessment of selected proteins was undertaken on fixed liver tissue. Cells were grown on chamber slides then fixed in methanol. Either standard avidin/biotin or immunofluorescence staining methods were performed. Details of antibodies used for each stains are as illustrated in Table 1. Picrosirius red staining was performed according to standard protocols.

Elastin Quantification. The entire liver section of each blinded slide was sequentially scanned at $\times$200 magnification, recording whether each field of view was positive or negative for elastin stained fibrotic scars and/or perisinusodial fibers (elastin positive vessel walls were excluded).

Image Analysis. Following elastin immunostaining or picrosirius red staining, the entire liver section of each blinded slide was sequentially scanned either at $\times$100 (mouse) or $\times$80 (rat) magnification. Stained areas were quantified by Adobe Photoshop CS2 and expressed as percentage of total pixels.

Immunoprecipitation and Casein Zymography. Immunoprecipitation was performed at 4°C using ice-cold buffers. Tissues were homogenized in lysis buffer (20 mM Tris HCl pH 8, 137 mM NaCl, 10% glycerol, 1% Triton X-100). Protein concentration was determined by Bradford Assay and equal amounts (500 μg) were diluted in 500 μL intraperitoneal lysis buffer and mixed with either anti-MMP-12 (Abcam) or anti TIMP-1 (ClonTech) at a final concentration of 1 μg/mL and rotated overnight. Then 100 μL of MagnaBind goat antirabbit IgG (Thermo, UK) or antimouse IgG1 Magnetic Particles - DM BD IMag (BD Biosciences) were added and rotated for 1 hour. Beads were magnetically separated for 8 minutes and supernatants were kept aside and equal volumes (20 μL) were used in western blot analysis for GAPDH to confirm initial equal protein amounts. Separated beads were washed 2 $\times$ 5 minutes in intraperitoneal lysis buffer. Samples were then resuspended in 25 μL zymography sample buffer (62.5 mM Tris-HCl, pH 6.8, 4% SDS, 25% glycerol, 0.01% Bromophenol Blue).

Casein zymography was performed according to Poppelmann et al.[26] with minor modifications. In short, samples were subjected to sodium dodecyl sulfate-polyacrylamide gel electrophoresis (SDS-PAGE) on a 12% gel containing 0.25% w/v skimmed milk powder. Following electrophoresis, gels were rinsed in deionized water and renatured in 2.5% Triton X-100 for 4 hours before incubation in activity buffer (50 mM Tris, 200 mM NaCl, 5 mM $CaCl_2$, 0.02% Brij-35, pH 7.5) at 37°C for 72 hours. Subsequently, the gel was stained in SimplyBlue SafeStain (Invitrogen) before destaining in water. Proteolytic activity was detected as destained bands against a background of Coomassie-stained casein.

Statistical Analysis. All data are expressed as mean $\pm$ standard deviation (SD). Statistical analysis was performed using SPSS software. To ensure normality and equality of variances, the data were log-transformed prior to analysis. Following transformation the groups were compared using the test indicated in each figure legend.

Results

Elastin Is a Feature of Fibrotic Scars. As we have previously described, administration of CCl_4 to rats for either 4 or 8 weeks leads to reversible fibrosis and early cirrhosis, respectively, whereas 12 weeks administration leads to micronodular cirrhosis.[4] Picrosirius red staining of rat liver tissue after CCl_4 administration showed increasing accumulation of collagen, detectable following 4, 8, and 12 weeks of injury (Fig. 1A1-4). Histomorphometric analysis (Fig. 1A5) confirmed the observation and showed significant increase in staining

15273350, 2012, 6, Downloaded from https://onlinelibrary.wiley.com/doi/10.1002/hep.25567, Wiley Online Library on [24/10/2025]. See the Terms and Conditions (https://onlinelibrary.wiley.com/terms-and-conditions) on Wiley Online Library for rules of use; OA articles are governed by the applicable Creative Commons License

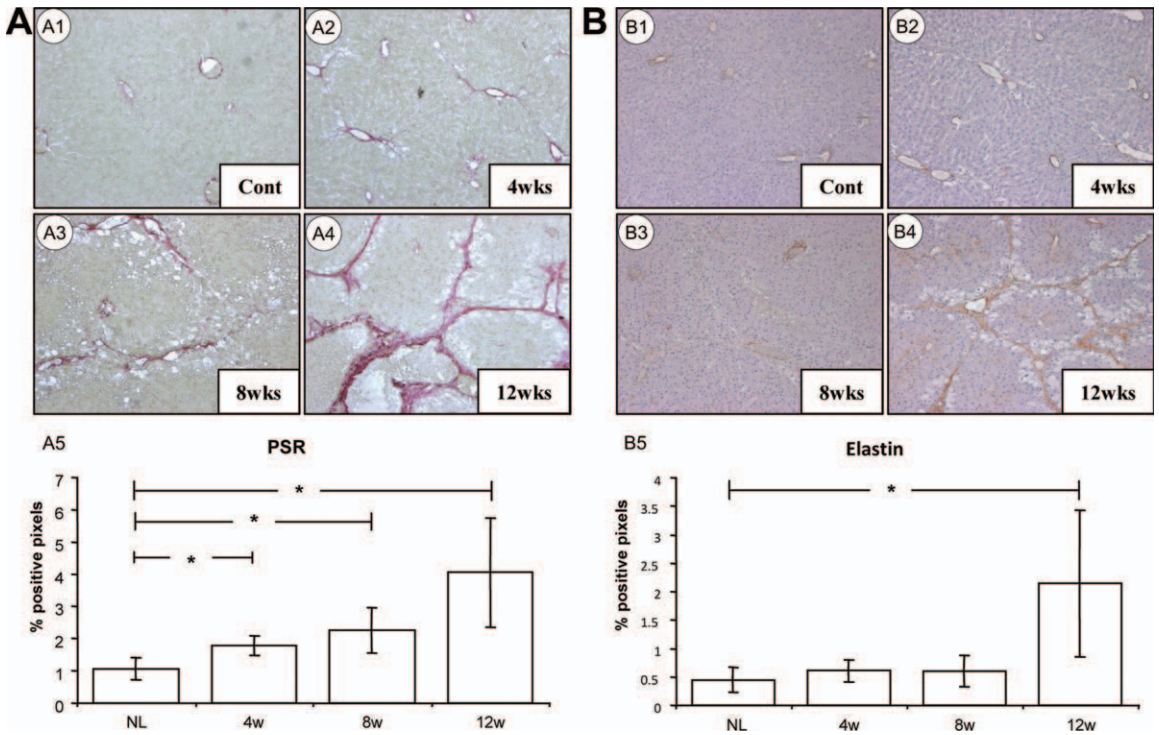

Fig. 1. Elastin is enriched in fibrotic scars. A: Representative pictures and image analysis of immunostaining for picrosirius red staining (A1-5) and elastin (B1-5). Original magnification ×80. In each panel, 1: Control, 2: 4 weeks CCl_4, 3: 8 weeks CCl_4, 4: 12 weeks CCl_4, 5: histomorphometric analysis of stained sections, expressed as percentage of positive pixels. Analysis of variance (ANOVA) followed by Dunnett's post-hoc test (n = 4-7).

at all timepoints, expressed as percentage of positive pixels: 1.06 ± 0.32 (normal liver, NL) 1.78 ± 0.30 (4 weeks $P = 0.019$ versus NL); 2.20 ± 0.73, (8 weeks $P = 0.001$), and 3.81 ± 1.62 (12 weeks $P < 0.001$).

In contrast, an increase in elastin deposition was only observed in relatively advanced fibrosis (Fig. 1B1-4). Histomorphometric analysis showed that only livers with established fibrosis had an increase in positive staining (0.44 ± 0.22 NL); 0.60 ± 0. 0.19 (4 weeks $P = 0.625$ versus NL); 0.59 ± 0.28, (8 weeks $P = 0.858$), and 3.81 ± 1.2 (12 weeks $P = 0.002$) (Fig. 1B5). The calculated ratio between PSR and elastin staining only raised above baseline after 12 weeks CCl_4 administration.

Tropoelastin Synthesis Is Increased upon CCl_4 Administration. The observation that elastin accumulates in fibrotic scars in advanced experimental cirrhosis poses a question whether the mechanism of elastin deposition is the result of an increase in synthesis, a failure of degradation, or both. To investigate, we analyzed whole tissue tropoelastin messenger RNA (mRNA) expression by way of quantitative reverse-transcription polymerase chain reaction (qPCR). Figure 2A shows tropoelastin transcription levels in the rat liver treated with CCl_4 as described above. At peak fibrosis, increasing duration of injury resulted in increasing tropoelastin expression (expressed as fold induction compared with NL): 4.2 ± 1.19 ($P = 0.017$), 8.5 ± 2.9 ($P < 0.001$), and 9.5 ± 2.7 ($P < 0.001$) times greater than normal liver for 4, 8, and 12 weeks, respectively.

Western blot analysis confirmed the observation (Fig. 2B,C), showing higher tropoelastin was present in advanced fibrosis. Thus, elastin is strongly expressed from the onset of injury but, in contrast to collagen I,[23] only accumulates late, suggesting it is regulated by degradation during injury.

To confirm the expression of elastin, immunocytochemistry analysis (Fig. 2D) of primary hepatic myofibroblasts was undertaken and indicated that these cells are positive for elastin, in keeping with previous studies.[27]

Ratio Between MMP-12 and TIMP-1 Is Altered in Liver Fibrosis. Given that expression of elastin begins earlier than its accumulation in the tissue, we investigated whether this might be mediated by alterations in elastin degradation. Therefore, we set to assess the two main enzymes responsible for elastin degradation (NE and MMP-12). NE was not detected in diseased rat livers at any timepoint, using qPCR or

15273350, 2012, 6, Downloaded from https://onlinelibrary.wiley.com/doi/10.1002/hep.25567, Wiley Online Library on [24/10/2025]. See the Terms and Conditions (https://onlinelibrary.wiley.com/terms-and-conditions) on Wiley Online Library for rules of use; OA articles are governed by the applicable Creative Commons License

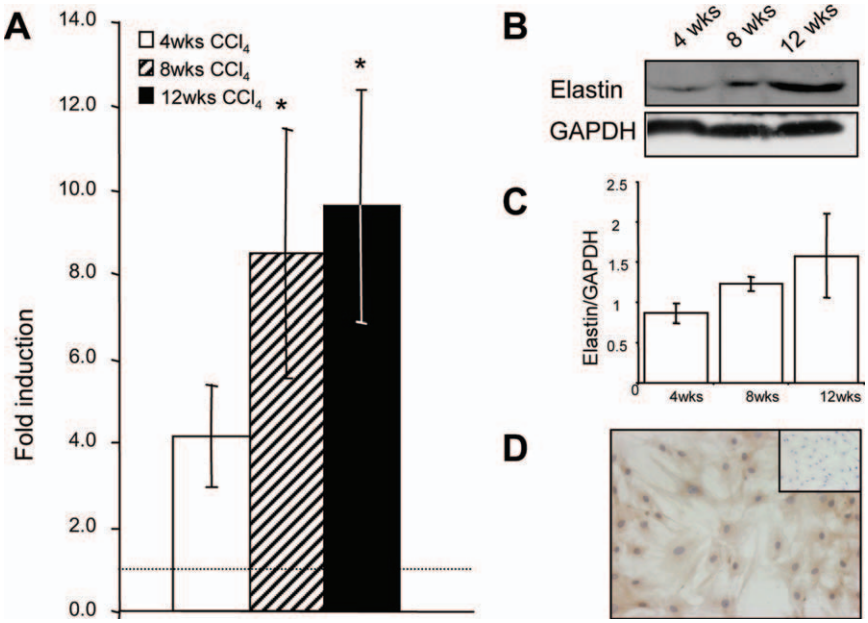

Fig. 2. Tropoelastin is up-regulated at peak fibrosis. A: Tropoelastin mRNA expression in rat liver after 4 (open bars), 8 (striped bars), or 12 (closed bars) weeks of CCl_4 injury. Expression was normalized to 18s and expressed as fold induction from noninjured liver. Samples were compared using a two-tailed ANOVA followed by a Dunnett's post-hoc test (n = 3-4). (B,C) Representative western blot analysis of elastin in rat after 4, 8, or 12 weeks of CCl_4 injury. Graph (C) shows densitometric analysis normalized to GAPDH. Kruskal-Wallis test ($P = 0.06$, n = 3). (D) Rat primary HSCs stained for tropoelastin (negative control inset) Original magnification ×200.

western blot analysis (data not shown). Neutrophil elastase was detectable in qPCR in mouse liver, but at a low and constant level (Fig. 4B4). Consequently, we focused on MMP-12.

CCl_4 administration for 4 weeks caused a minor increase in *MMP-12* gene expression that was not statistically significant ($P = 0.066$) (Fig. 3A). Conversely, both 8 and 12 weeks injury with CCL_4 caused increased MMP-12 expression, 6.2 ± 5.4; ($P = 0.007$) and 11.2 ± 5.1, ($P < 0.001$) times compared with normal liver, respectively. Western blot analysis indicated that levels of MMP-12 were modestly increased with injury duration as shown in Fig. 3B. Specificity of bands was confirmed with two different antibodies and competition with immunizing blocking peptide. After densitometric analysis corrected for GAPDH expression, the expression of MMP-12 showed no significant changes across all groups (data not shown). Given the tightly regulated activity of MMPs,[9,10] it was important to detect whether active MMP-12 was present.

One of the main factors in determining MMP activity is the ratio with their tissue inhibitors, especially TIMP-1. TIMP-1 mRNA and protein (Fig. 3B) were increased after 8 and 12 weeks injury. In order to establish the degree of inhibition of MMP-12 by TIMP-1 in our model system, we coimmunoprecipitated the two proteins and analyzed the samples by zymography. After immunoprecipitation of MMP-12, casein zymography (Fig. 3C) showed a similar pattern to the samples used for western blot, indicating even efficiency of precipitation. Additionally, when we immunoprecipitated TIMP-1 and performed casein zymography (Fig. 3C) the signal increased through 4 to 8 and 12 weeks (Fig. 3C), indicating that there is increasing amounts of TIMP-1 bound to MMP-12 in increasingly fibrotic liver. Thus, MMP-12 is present in the liver but held in check by noncovalent binding to TIMP-1 with increasing duration of liver injury.

Taken together, these data strongly suggest that the elastin content in scars is regulated by MMP-12-mediated degradation, with active MMP-12 being inhibited by increased interaction with TIMP-1 with worsening fibrosis *in vivo*. Previous work by Yoshiji et al.[10,28] using a TIMP-1 overexpression, however, suggests that the Timp-1 inhibition may not be maximal and MMP-mediated degradation still occurs in remodeling during progressive fibrosis.

Macrophages Are the Main Source of MMP-12. MMP-12 has been reported to be expressed by macrophages.[29] We confirmed this by immunocytochemistry on human monocyte-derived macrophages stained for both MMP-12 and the macrophage marker CD-68 (Fig. 4A1-2); 100% of the cells were positive for both proteins. To define which cells express MMP-12 *in vivo*, we stained serial sections of rat tissue for MMP-12 and CD-68 (Fig. 4A3-4). We found that the cells positive for MMP-12 were macrophages but that only a proportion of the CD-68-positive macrophages were also positive for MMP-12.

To confirm the macrophage origin of MMP-12, we used the transgenic mouse CD11b-DTR in which macrophages can be selectively depleted as described.[22] These mice show a 50% decrease in macrophage populations and increased accumulation of elastin compared with WT mice after CCl_4 administration.

15273350, 2012, 6, Downloaded from https://onlinelibrary.wiley.com/doi/10.1002/hep.25567, Wiley Online Library on [24/10/2025]. See the Terms and Conditions (https://onlinelibrary.wiley.com/terms-and-conditions) on Wiley Online Library for rules of use; OA articles are governed by the applicable Creative Commons License

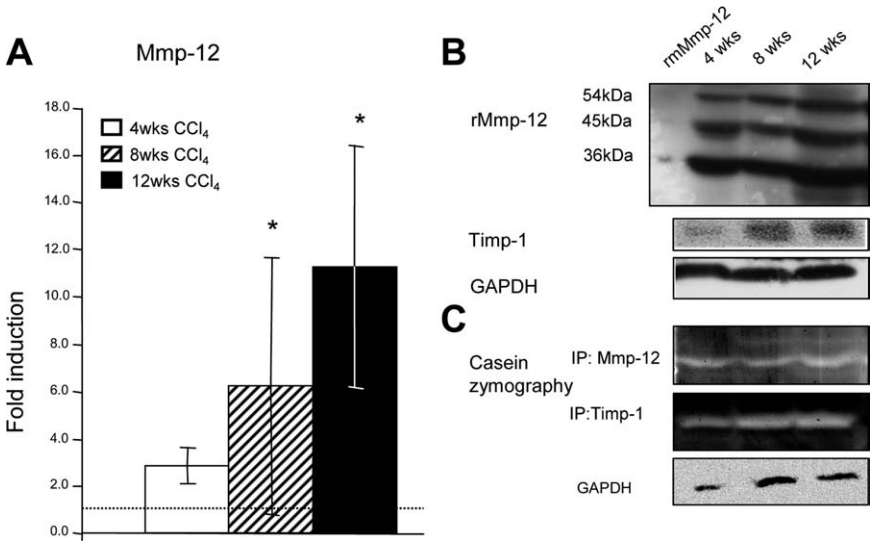

Fig. 3. rMmp-12 is up-regulated at peak fibrosis at the mRNA level but not at the protein level. (A) MMP-12 mRNA expression in rat liver after 4 (open bars), 8 (striped bars), or 12 (closed bars) weeks of CCl_4 injury. Expression was normalized to 18s and expressed as fold induction from noninjured liver. Samples were compared using a two-tailed ANOVA followed by a Dunnett's post-hoc test. n = 3, 4. (B) western blot analysis for rat MMP-12, TIMP-1 and GAPDH at the indicated time of CCl_4 injury. (C) Coimmunoprecipitation of MMP-12 and TIMP-1. Samples were precipitated for either MMP-12 or Timp-1 and underwent casein zymography assay. Supernatants of the immunoprecipitations were used in western blot analysis for GAPDH.

Staining of liver following macrophage depletion showed a significant decrease in MMP-12-positive cells (Fig. 4B1-3). qPCR analysis of these tissues (Fig. 4B4) showed no significant changes in the expression of either tropoelastin or neutrophil elastase, whereas MMP-12 expression was significantly decreased.

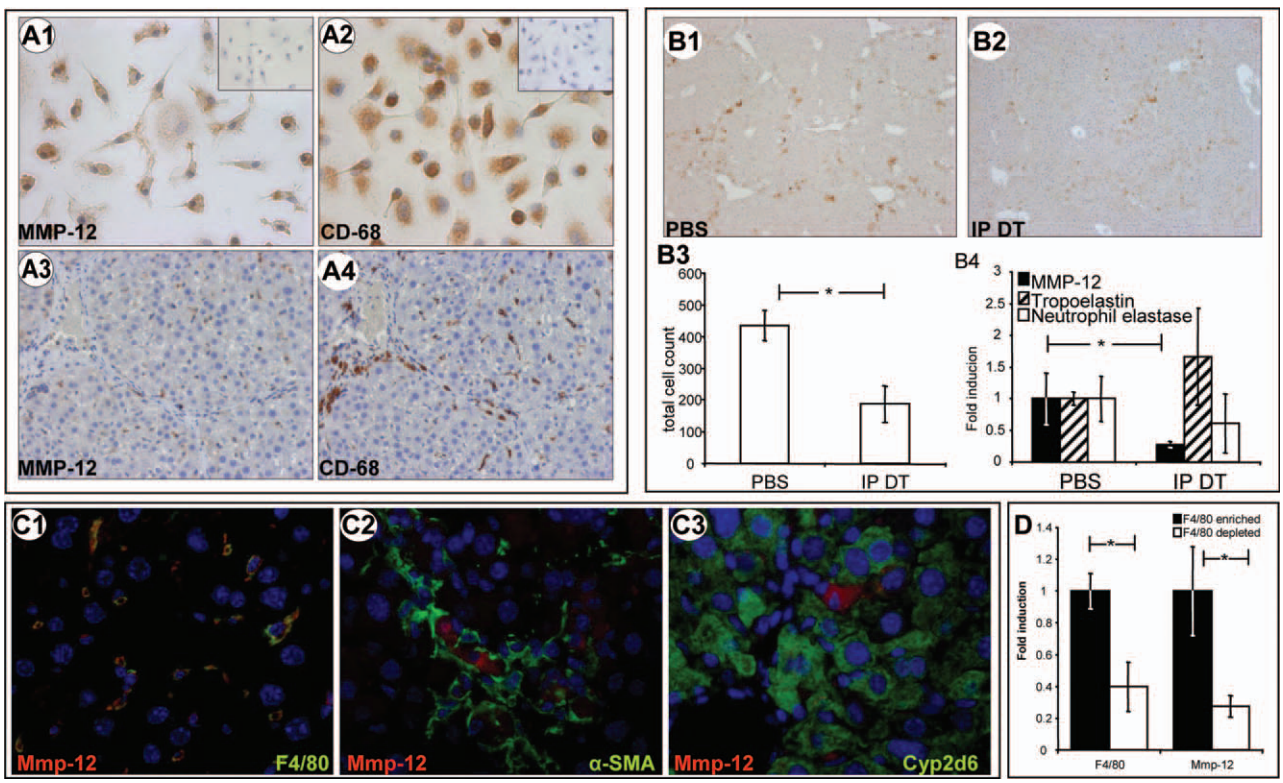

Fig. 4. Mmp-12 is expressed by macrophages. (A) Human monocyte-derived macrophages were stained for MMP-12 (A1) and the macrophage marker CD-68 (A2) and counterstained for hematoxylin (original magnification ×320). Liver tissue from rats exposed to CCl_4 for 6 weeks were harvested at peak fibrosis. Formalin-fixed, paraffin-embedded sections were immunostained for either MMP-12 (A3) or the macrophage marker CD-68 (A4). Sections were counterstained with hematoxylin (blue nuclei) (original magnification ×200). (B1-2) Representative liver sections from CD11b-DTR mice treated with CCl_4 for 4 weeks and injected with DT stained for MMP-12. (B3) Total cell counts of MMP-12 positive cells in 10 sequential fields per slide (original magnification ×200; n = 3). (B4) Relative mRNA expression of MMP-12 (closed bars), tropoelastin (striped bars), and NE (open bars). Expression was normalized to 18s. Samples were compared using a two-tailed Kruskal-Wallis test (n = 3-4). (C) Formalin-fixed, paraffin-embedded sections immunostained MMP-12 and the cell markers F4/80 (C1, macrophages), α-SMA (C2, myofibroblasts), and Cyp2d6 (C3, hepatocytes), showing colocalization of MMP-12 solely to F4/80. (D) F4/80 and MMP-12 mRNA levels in F4/80-enriched and -depleted cell populations from mouse liver exposed to 4 weeks CCl_4.

15273350, 2012, 6, Downloaded from https://onlinelibrary.wiley.com/doi/10.1002/hep.25567, Wiley Online Library on [24/10/2025]. See the Terms and Conditions (https://onlinelibrary.wiley.com/terms-and-conditions) on Wiley Online Library for rules of use; OA articles are governed by the applicable Creative Commons License

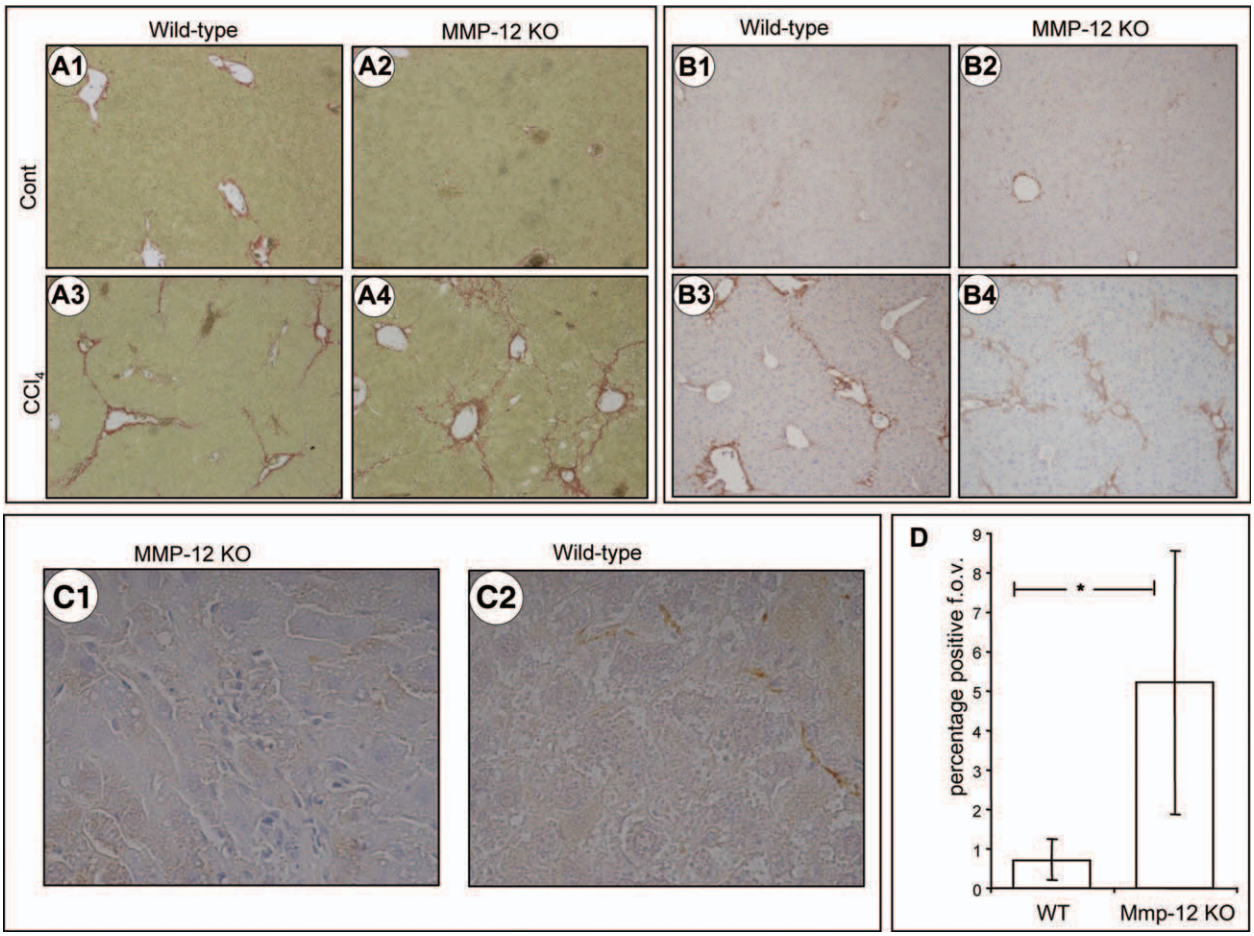

Fig. 5. CCl_4 causes similar injury to the liver in WT and MMP-$12^{-/-}$ mice, but accumulation of perisinusoidal elastin only in MMP-$12^{-/-}$ mice. Representative pictures of picrosirius red staining (A1-4) and immunostaining for collagen I (B1-4). Original magnification ×100. In each panel, 1: WT control, 2: MMP-$12^{-/-}$ control, 3: WT + CCl_4, 4: MMP-$12^{-/-}$ + CCl_4. (C1-2) Elastin immunostaining in WT (C1) and MMP-$12^{-/-}$ after CCl_4 administration (original magnification ×320). (D) Percentage of power fields positive for perisinusoidal elastin, Samples were compared using a two-tailed Kruskal-Wallis test; n = 6.

To further confirm that macrophages are the major hepatic source of MMP-12, we costained mouse liver after CCl_4 injury for MMP-12 and key liver cell markers. Figure 4C shows representative immunofluorescence images of MMP-12 and the macrophage marker F4/80 (C1), alpha-smooth muscle actin (α-SMA) (for myofibroblasts, C2) and Cyp2D6 (hepatocytes, C3). MMP-12 was exclusively colocalized to F4/80-positive cells, confirming macrophages as a source of MMP-12.

To confirm MMP-12 expression in F4/80-positive cells, we isolated hepatic macrophages from a short model of CCl_4 injury. Following isolation of hepatic macrophages, the purity of F4/80-enriched and F4/80-depleted populations was assessed by qPCR (Fig. 4D). Quantitation of MMP-12 mRNA showed that the macrophage-enriched cell population had higher expression of MMP-12 than the macrophage-depleted population (Fig. 4D).

Overall, this demonstrates that MMP-12 in different species is expressed by a population of hepatic macrophages in the fibrotic liver and mechanistically linked to elastin degradation.

MMP-12 Deletion Is Associated with Liver Accumulation of Elastin. In order to define mechanistically the role of MMP-12 and elastin degradation in the development of fibrosis, we exposed MMP-$12^{-/-}$ mice and C57Bl/6 WT controls to either CCl_4 or olive oil for 12 weeks. Animals were sacrificed 48 hours after the last injection. Serum markers of hepatocyte damage (alanine aminotransferase [ALT] and aspartate aminotransferase [AST]) in the knockout were comparable to those of the WT (Supporting data). Picrosirius red staining and collagen I immunohistochemistry indicated that CCl_4 induced an identical degree of fibrosis in the WT and MMP-$12^{-/-}$ animals (Fig. 5A,B, respectively). Quantification of either staining by image analysis did not show a significant

15273350, 2012, 6, Downloaded from https://onlinelibrary.wiley.com/doi/10.1002/hep.25567, Wiley Online Library on [24/10/2025]. See the Terms and Conditions (https://onlinelibrary.wiley.com/terms-and-conditions) on Wiley Online Library for rules of use; OA articles are governed by the applicable Creative Commons License

difference between the groups (data not shown). Despite the fact that no difference in overall fibrosis could be detected, immunohistochemistry for elastin did show a subtle phenotypic difference between the WT and MMP-12 null mice. Figure 5C shows high-power representative images of elastin immunohistochemistry in the WT and the knockout after CCl_4 administration. On close examination the MMP-$12^{-/-}$ mice showed clear evidence of perisinusoidal elastin that was not detected in the WT controls. The quantification by percentage of positive fields containing elastin in Fig. 5D shows that there was a significant increase of perisinusoidal elastin in the MMP-$12^{-/-}$ fibrotic livers ($P = 0.004$).

Because elastin is a late feature of fibrosis, we hypothesized that the relatively short duration of the injury highlighted a subtle phenotype only. We determined that a model of protracted low-level injury was necessary to more robustly highlight the role of MMP-12 in elastin turnover. Thus, MMP-$12^{-/-}$ mice and C57Bl/6 WT controls were given dietary TAA (600 mg/L in drinking water) for 52 weeks. Figure 6A shows representative images of elastin immunostaining in the WT and the knockout mice in undamaged liver and after TAA administration. Quantification by image analysis showed that TAA significantly increased elastin deposition in the knockout ($P = 0.015$), but not in the WT (Fig. 6A5). Interestingly, Picrosirius Red (Fig. 6B) staining showed that TAA increased bridging fibrosis both in the WT and the knockout ($P = 0.001$ and $P < 0.001$, respectively), but the latter showed significantly higher levels of bridging fibrosis ($P = 0.002$), suggesting that a failure to degrade elastin would itself enhance the development of fibrosis. Importantly, this phenotypic difference was not accompanied by compensatory changes in tropoelastin gene expression or expression of other relevant MMPs and TIMPs (Fig. 6C). Additionally, no differences in activation were seen in either MMP-2 or MMP-9 (Fig. 6D) after TAA administration, once again highlighting the role of MMP-12 in regulating elastin levels in the fibrotic liver at the level of degradation.

Discussion

We have presented evidence in these and other studies that the presence of elastin within hepatic scars is associated with duration of injury.[22] Our data demonstrate that elastin accumulation, rather than being only the result of excessive secretion, also results from a failure of elastin degradation. With increasing duration of fibrotic injury there is a modest increase in expression of tropoelastin and MMP-12. However, as we have shown in previous studies[23] and by using immunoprecipitation in the work reported here, there is a concurrent increase in expression of TIMPs 1 and 2, which results in significant inhibition of MMP activity and a consequent failure of elastin degradation. This is shown most directly by our studies immunoprecipitating MMP-12 by using an antibody to TIMP-1 as the bait and demonstrating increasing MMP-12 complexed to TIMP-1 during progressive fibrosis. TIMPs bind nonconvalently to MMP-12 and by casein zymography it is possible to demonstrate detectable evidence of elastase activity with separation of the complex. Thus, in a manner identical to that demonstrated by ourselves and Yoshiji et al.[10] with respect to collagen turnover, elastin turnover appears to be significantly but not entirely inhibited during progressive fibrosis leading to net matrix accumulation, but with limited remodeling still occurring as demonstrated by MMP-12 knockout models. This model is supported by the disparity between tropoelastin expression and elastin content of livers. Elastin is strongly expressed from the onset of injury but, in contrast to collagen I, only accumulates late, suggesting that degradation occurs during the early phases of injury.

The enzymes regulating elastin turnover in liver, indeed in any organ fibrosis, are incompletely defined in comparison to the collagenous component. After depleting macrophages in experimental liver fibrosis, there is an accumulation of elastin in the hepatic scar relative to controls in which macrophage numbers are maintained. Clearly these data point to macrophages as the major mediators of elastin degradation in liver fibrosis. Two prominent elastases have been implicated in elastin turnover in models of connective tissue biology: MMP-12 and NE. Interestingly, when we analyzed experimentally injured liver tissue from the rat and mouse NE expression was at the limit of PCR detection following CCl_4 or TAA treatment. Conversely, MMP-12 is present in the liver of injured animals, regulated with fibrotic injury and localized to macrophages within and adjacent to the hepatic scar. In contrast to MMP-13 and MMP-9, however, only a subset of hepatic macrophages express MMP-12. To definitively prove an association between MMP-12 and hepatic macrophages, we went on to quantitate MMP-12 expression before and after macrophage depletion and coimmunostaining for MMP-12 and key markers for selected cell types (F4/80, α-SMA, Cyp2d6). The reduction in MMP-12-positive cells following macrophage depletion and colocalization of Mmp-12 only to the macrophage marker F4/80

15273350, 2012, 6, Downloaded from https://onlinelibrary.wiley.com/doi/10.1002/hep.25567, Wiley Online Library on [24/10/2025]. See the Terms and Conditions (https://onlinelibrary.wiley.com/terms-and-conditions) on Wiley Online Library for rules of use; OA articles are governed by the applicable Creative Commons License

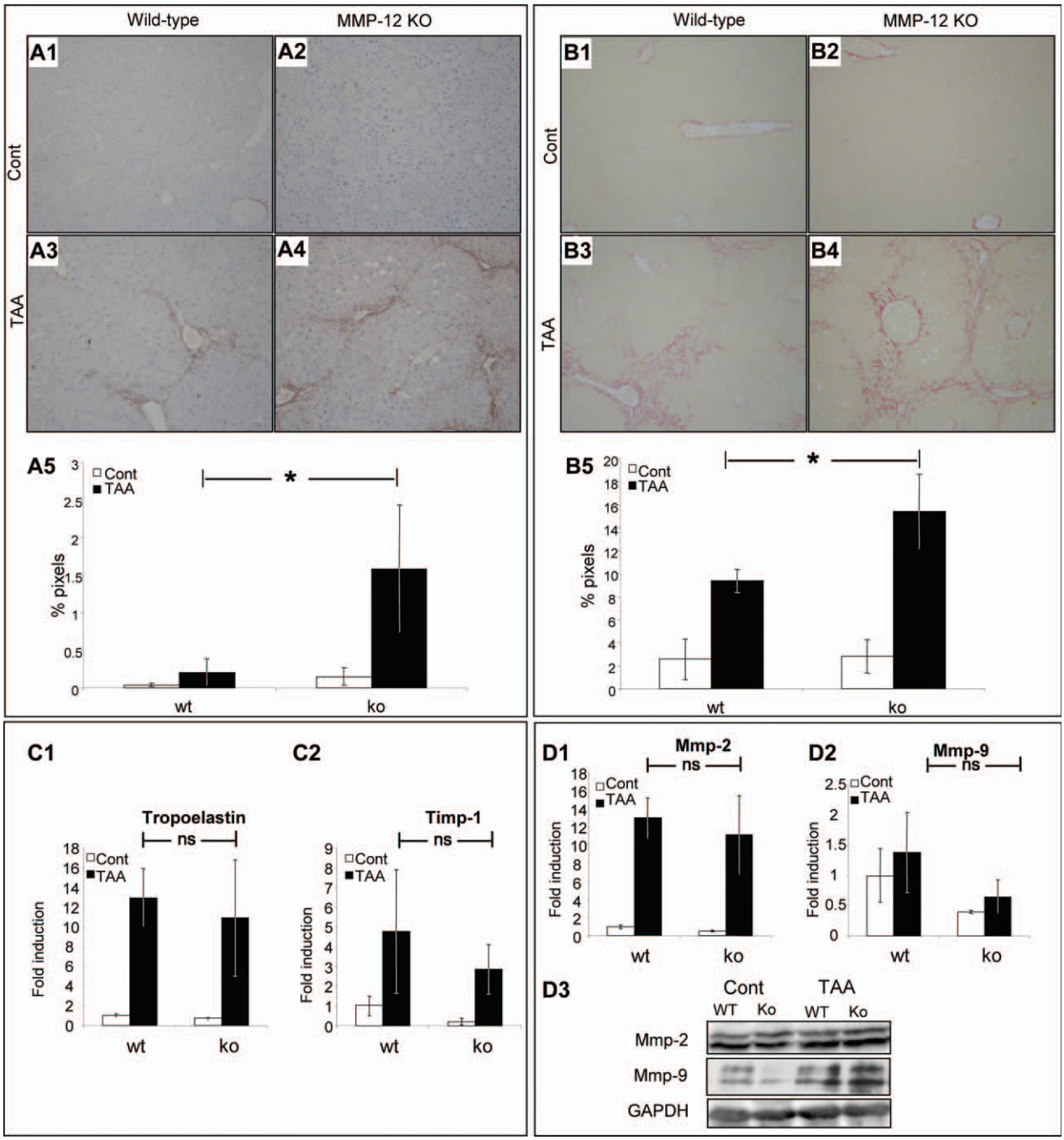

Fig. 6. MMP-12$^{-/-}$ mice develop more severe and elastin rich fibrosis after TAA. Representative pictures and image analysis of immunostaining for elastin (A1-4) and picrosirius red staining (B1-4). Original magnification ×100. In each panel, 1: WT control, 2: MMP-12$^{-/-}$ control, 3: WT + TAA (1 year), 4: MMP-12$^{-/-}$ + TAA (1 year), 5: histomorphometric analysis of stained sections, expressed as percentage of positive pixels. ANOVA followed by Tukeys's post-hoc test; n = 3-4. (C) mRNA expression of: tropoelastin (C1) and TIMP-1 (C2). (D) mRNA expression MMP-2 (D1) and MMP-9 (D2) in mouse liver after 1 year of oral TAA (closed bars) and age-matched controls. Expression was normalized to 18s and expressed as fold induction from noninjured liver. ANOVA followed by Tukeys's post-hoc test (n = 3-4). (D3) Western blot analysis for MMP-2, MMP-9, and loading control GAPDH.

significantly reinforce the evidence that it is macrophage-derived MMP-12 that mediates elastin turnover in experimental liver fibrosis.

Combined with our previous data showing the critical role of TIMP-1 in determining reversibility of liver fibrosis and the data demonstrating enhanced TIMP:MMP-12 complexing defined by immunoprecipitation in this study, our findings point to elastin also being regulated at the level of degradation in addition to synthesis in experimental liver fibrosis. To define, mechanistically, the role of MMP-12-mediated elastin turnover in liver fibrosis we went on to utilize MMP-12 knockout mice.

15273350, 2012, 6, Downloaded from https://onlinelibrary.wiley.com/doi/10.1002/hep.25567, Wiley Online Library on [24/10/2025]. See the Terms and Conditions (https://onlinelibrary.wiley.com/terms-and-conditions) on Wiley Online Library for rules of use; OA articles are governed by the applicable Creative Commons License

Given the difference between elastin expression and accumulation, we hypothesized that MMP-12 knockout mice would have a phenotype at progressive fibrosis, in contrast to MMP-13 (collagenase) knockout mice that show a similar degree of collagen deposition to the WT mice at peak injury.[23]

Our initial studies deployed the commonly used CCl_4-induced model of liver fibrosis. In this model we observed a clear-cut but subtle phenotype in the MMP-12$^{-/-}$ mice, in which in a significant proportion of fields there was evidence of a perisinusoidal and occasional linear accumulation of elastin, in comparison to WT controls. In keeping with the importance of duration of injury to elastin accumulation, exposure of mice to thioacetamide for 1 year resulted in a dramatic and extensive fibrosis, containing elastin and bordering on early cirrhosis. This model confirmed an accumulation of elastin in the MMP-12$^{-/-}$ that was dramatically enhanced relative to the WT controls. Importantly, neither model showed differences in elastin production between WT and knockout animals. Thus, our studies with the MMP-12 knockout, using two independent models of liver fibrosis, both of which demonstrate an accumulation of elastin in the knockout livers, provide evidence that a major regulatory step for elastin in liver fibrogenesis is at the level of degradation.

Interestingly, our studies using the MMP-12$^{-/-}$ also provide insights into the histological distribution of scar during fibrosis progression. Clearly, in the TAA model there was significantly enhanced elastin in the linear and bridging scars in knockout animals. Additionally, there was evidence of perisinusoidal elastin deposition in both genotypes, albeit more prominent in the MMP-12 null mice. A similar distribution of perisinusoidal elastin was also seen following CCl_4 administration in the knockout but not the WT animals. These data show a striking similarity to our previous studies of the rr mutant mouse which secretes a collagen not susceptible to MMP degradation.[30] In that model, prominent perisinusoidal collagen deposition was observed following induction of experimental fibrosis. Taken together, this suggests that the normal pattern of both elastin and collagen degradation as fibrosis remodels even in progressive disease is one in which perisinusoidal fibrosis is remodeled but there is relative resistance to degradation of the thicker and linear scars.

The other striking finding from long-term administration of TAA to the MMP-12$^{-/-}$ animals was the increased accumulation of collagen in knockout compared with WT mice. This raises a number of interesting mechanistic questions. MMP-12 has been shown to have direct collagenolytic activity,[31] and the observed differences may represent lack of this effect. However, one might have expected to see a similar difference in collagen deposition following chronic CCl_4 administration, which was not evident from our study. Furthermore, no compensatory increases in other MMPs in the MMP-12$^{-/-}$ mice were detected in our model, nor were changes in their global or activated protein levels as is described when other MMPs are deleted.[32,33]

We have presented cogent evidence that elastin accumulates in advanced liver injury but this occurs as a result of both synthesis and a failure of degradation. However, a level of degradation occurs and is mediated by MMP-12 derived from hepatic macrophages. Supporting this pathogenic model, MMP-12 knockout mice demonstrate significant elastin accumulation, highlighting mechanistically the importance of this enzyme in mediating elastin turnover during experimental fibrosis. These observations have important implications for the design of antifibrotic therapies.

References

1. Office for National Statistics. Mortality Statistics, Deaths registered in 2008, DR_08. 2008.
2. Benyon RC, Iredale JP. Is liver fibrosis reversible? Gut 2000;46: 443-446.
3. Iredale JP, Benyon RC, Pickering J, McCullen M, Northrop M, Pawley S, et al. Mechanisms of spontaneous resolution of rat liver fibrosis. Hepatic stellate cell apoptosis and reduced hepatic expression of metalloproteinase inhibitors. J Clin Invest 1998;102:538-549.
4. Issa R, Zhou X, Constandinou CM, Fallowfield J, Millward-Sadler H, Gaca MD, et al. Spontaneous recovery from micronodular cirrhosis: evidence for incomplete resolution associated with matrix cross-linking. Gastroenterology 2004;126:1795-1808.
5. Iredale JP. Hepatic stellate cell behavior during resolution of liver injury. Semin Liver Dis 2001;21:427-436.
6. Lorena D, Darby IA, Reinhardt DP, Sapin V, Rosenbaum J, Desmouliere A. Fibrillin-1 expression in normal and fibrotic rat liver and in cultured hepatic fibroblastic cells: modulation by mechanical stress and role in cell adhesion. Lab Invest 2004;84:203-212.
7. Kanta J, Dooley S, Delvoux B, Breuer S, D'Amico T, Gressner AM. Tropoelastin expression is up-regulated during activation of hepatic stellate cells and in the livers of CCl4-cirrhotic rats. Liver 2002;22: 220-227.
8. Friedman SL. Hepatic stellate cells: protean, multifunctional, and enigmatic cells of the liver. Phys Rev 2008;88:125-172.
9. Ramachandran P, Iredale JP. Reversibility of liver fibrosis. Ann Hepatol 2009;8:283-291.
10. Yoshiji H, Kuriyama S, Yoshii J, Ikenaka Y, Noguchi R, Nakatani T, et al. Tissue inhibitor of metalloproteinases-1 attenuates spontaneous liver fibrosis resolution in the Transgenic mouse. HEPATOLOGY 2002;36: 850-860.
11. Reiser K, Mccormick RJ, Rucker RB. Enzymatic and nonenzymatic cross-linking of collagen and elastin. FASEB J 1992;6:2439-2449.
12. Yanagisawa H, Davis EC. Unraveling the mechanism of elastic fiber assembly: the roles of short fibulins. Int J Biochem Cell Biol 2010;42: 1084-1093.

15273350, 2012, 6, Downloaded from https://onlinelibrary.wiley.com/doi/10.1002/hep.25567, Wiley Online Library on [24/10/2025]. See the Terms and Conditions (https://onlinelibrary.wiley.com/terms-and-conditions) on Wiley Online Library for rules of use; OA articles are governed by the applicable Creative Commons License

13. Rosenbloom J, Harsch M, Cywinski A. Evidence that tropoelastin is the primary precursor in elastin biosynthesis. J Biol Chem 1980;255: 100-106.
14. Grenard P, Bresson-Hadni S, El Alaoui S, Chevallier M, Vuitton DA, Ricard-Blum S. Transglutaminase-mediated cross-linking is involved in the stabilization of extracellular matrix in human liver fibrosis. J Hepatol 2001;35:367-375.
15. Hornstra IK, Birge S, Starcher B, Bailey AJ, Mecham RP, Shapiro SD. Lysyl oxidase is required for vascular and diaphragmatic development in mice. J Biol Chem 2003;278:14387-14393.
16. Bedossa P, Lemaigre G, Paraf F, Martin E. Deposition and remodeling of elastic fibers in chronic hepatitis. Virchows Arch A Pathol Anat Histopathol 1990;417:159-162.
17. Liban E, Ungar H. Elastosis in fibrotic and cirrhotic processes of the liver. Arch Pathol 1959;68:331-341.
18. Shikata T, Sakai T. Elastogenesis in liver. Acta Pathol Jpn 1974;24: 21-31.
19. Kanta J, Velebny V, Mergancova J, Ettlerova E, Chlumska A. Elastin content in human fibrotic and cirrhotic liver. Sb Ved Pr Lek Fak Karlovy Univerzity Hradci Kralove 1990;33:5.
20. Shapiro SD, Kobayashi DK, Ley TJ. Cloning and characterization of a unique elastolytic metalloproteinase produced by human alveolar macrophages. J Biol Chem 1993;268:23824-23829.
21. MonetKuntz C, Cuvelier A, Sarafan N, Martin JP. Metalloelastase expression in a mouse macrophage cell line — regulation by 4 beta-phorbol 12-myristate 13-acetate, lipopolysaccharide and dexamethasone. Eur J Biochem 1997;247:588-595.
22. Duffield JS, Forbes SJ, Constandinou CM, Clay S, Partolina M, Vuthoori S, et al. Selective depletion of macrophages reveals distinct, opposing roles during liver injury and repair. J Clin Invest 2005;115: 56-65.
23. Fallowfield JA, Mizuno M, Kendall TJ, Constandinou CM, Benyon RC, Duffield JS, et al. Scar-associated macrophages are a major source of hepatic matrix metalloproteinase-13 and facilitate the resolution of murine hepatic fibrosis. J Immunol 2007;178:5288-5295.
24. Issa R, Williams E, Trim N, Kendall T, Arthur MJ, Reichen J, et al. Apoptosis of hepatic stellate cells: involvement in resolution of biliary fibrosis and regulation by soluble growth factors. Gut 2001;48:548-557.
25. MacKinnon AC, Farnworth SL, Hodkinson PS, Henderson NC, Atkinson KM, Leffler H, et al. Regulation of alternative macrophage activation by galectin-3. J Immunol 2008;180:2650-2658.
26. Poppelmann M, Becker WM, Petersen A. Combination of zymography and immunodetection to analyze proteins in complex culture supernatants. Electrophoresis 2002;23:993-997.
27. Guyot C, Combe C, Desmouliere A. The common bile duct ligation in rat: a relevant in vivo model to study the role of mechanical stress on cell and matrix behaviour. Histochem Cell Biol 2006;126:517-523.
28. Yoshiji H, Kuriyama S, Miyamoto Y, Thorgeirsson UP, Gomez DE, Kawata M, et al. Tissue inhibitor of metalloproteinases-1 promotes liver fibrosis development in a transgenic mouse model. HEPATOLOGY 2000;32:1248-1254.
29. Belaaouaj A, Shipley JM, Kobayashi DK, Zimonjic DB, Popescu N, Silverman GA, et al. Human macrophage metalloelastase — genomic organization, chromosomal location, gene linkage, and tissue-specific expression. J Biol Chem 1995;270:14568-14575.
30. Zhou XY, Jamil A, Nash A, Chan J, Trim N, Iredale JP, et al. Impaired proteolysis of collagen I inhibits proliferation of hepatic stellate cells — implications for regulation of liver fibrosis. J Biol Chem 2006;281: 39757-39765.
31. Taddese S, Jung MC, Ihling C, Heinz A, Neubert RHH, Schmelzer CEH. MMP-12 catalytic domain recognizes and cleaves at multiple sites in human skin collagen type I and type III. Biochim Biophys Acta Proteins Proteom 2010;1804:731-739.
32. Ikonomidis JS, Barbour JR, Amani Z, Stroud RE, Herron AR, McClister DM, et al. Effects of deletion of the matrix metalloproteinase 9 gene on development of murine thoracic aortic aneurysms. Circulation 2005;112:I242-I248.
33. Longo GM, Xiong WF, Greiner TC, Zhao Y, Fiotti N, Baxter BT. Matrix metalloproteinases 2 and 9 work in concert to produce aortic aneurysms. J Clin Invest 2002;110:625-632.

15273350, 2012, 6, Downloaded from https://onlinelibrary.wiley.com/doi/10.1002/hep.25567, Wiley Online Library on [24/10/2025]. See the Terms and Conditions (https://onlinelibrary.wiley.com/terms-and-conditions) on Wiley Online Library for rules of use; OA articles are governed by the applicable Creative Commons License